POLITECNICO DI TORINO
Repository ISTITUZIONALE

Homogenization Techniques for Nanocomposites: A Comprehensive Review

Original
Homogenization Techniques for Nanocomposites: A Comprehensive Review / Angelini, D., Cestino, E., Piana, P., Mallamo, F.. - (2025), pp. 149-163. (DRaF 2024 Ischia (NA) June 17–21, 2024) [10.1007/978-3-031-77697-7_17].

Availability:
This version is available at: 11583/2995978 since: 2026-05-19T07:18:52Z

Publisher:
Springer

Published
DOI:10.1007/978-3-031-77697-7_17

Terms of use:

This article is made available under terms and conditions as specified in the corresponding bibliographic description in the repository

Publisher copyright
Springer postprint/Author's Accepted Manuscript

This version of the article has been accepted for publication, after peer review (when applicable) and is subject to Springer Nature's AM terms of use, but is not the Version of Record and does not reflect post-acceptance improvements, or any corrections. The Version of Record is available online at: http://dx.doi.org/10.1007/978-3-031-77697-7_17

(Article begins on next page)

27 November 2026

HOMOGENIZATION TECHNIQUES FOR NANOCOMPOSITES: A COMPREHENSIVE REVIEW

D. Angelini[1[0009-0001-1585-7037]], E. Cestino[1[0000-0003-4842-3320]], P. Piana[2], F. Mallamo[2]

[1] Politecnico di Torino, C.so Duca degli Abruzzi 24, 10129, Turin, Italy
[2] FEV Italy s.r.l., Via Livorno 60, 10144, Turin, Italy
davide.angelini@polito.it

Abstract. The study analyzes the development of analytical models for the reinforcement of structures using nanomaterials. Initially, it introduces the "Surface stress" phenomenon within the context of composite materials. In fact, nanocomposites show distinct characteristics compared to traditional composites due to the high surface-to-volume ratio at the nanoscale, which significantly influences the mechanical properties. Secondly, the research explores the Eshelby Tensor for a homogeneous solid with inclusions. Thirdly, various homogenization methods are compared, such as the Mori-Tanaka method, the self-consistent method with Eshelby Tensor and the refined Mori-Tanaka method for determining the effective stiffness tensor of nanocomposites. Fourthly, the introduction of "interface stress" between matrix and nanomaterials is analyzed. All the models are compared based on values of experimental results; moreover, a comparison with traditional composite techniques is performed. Overall, this work provides a detailed analytical framework for understanding and predicting the behavior of nanocomposites, integrating advanced mathematical models to account for the unique effects observed at the nanoscale.

Keywords: nanomaterials, nanocomposites, RVE, homogenization, Molecular Dynamics, Mori-Tanaka, multiscale

1 Introduction

1.1 Features of nanoscale materials

Nanocomposites are composite materials in which at least one characteristic dimension of the filler ranges from 1 to 100 nm [1]. At these scales, materials exhibit properties different from those observed in bulk materials [2]. When the matrix is composed of polymers, the materials are referred to as Polymer Matrix Nanocomposites (PMNCs); if the matrix is metallic, they are called Metal Matrix Nanocomposites (MMNCs). In bulk materials, a significant portion of the material resides within the particles themselves; however, nanomaterials have **a high surface-to-volume ratio** [3]. Consequently, surface atoms with dangling bonds exhibit

quantum mechanical behaviors [4], but also new mechanical properties emerge [5], such as the condition of surface stress [6].

Consider a simple model of two-dimensional metal nanoparticles from [6]. An atom *P* located within the material experiences equal forces in both the *X* and *Y* directions (Figure 1a, left). In contrast, a surface atom experiences an unbalanced force along the X-axis and is therefore subjected to an attractive force from the interior of the particle (Figure 1a, right). As a result, a condition of surface tension arises [6]. In the context of MMNCs, the lattice mismatch between the nanofiller and the external matrix can amplify this condition, leading to localized stresses. In practical cases, the interface is more complex; there is no clear boundary between the matrix and the filler [7].

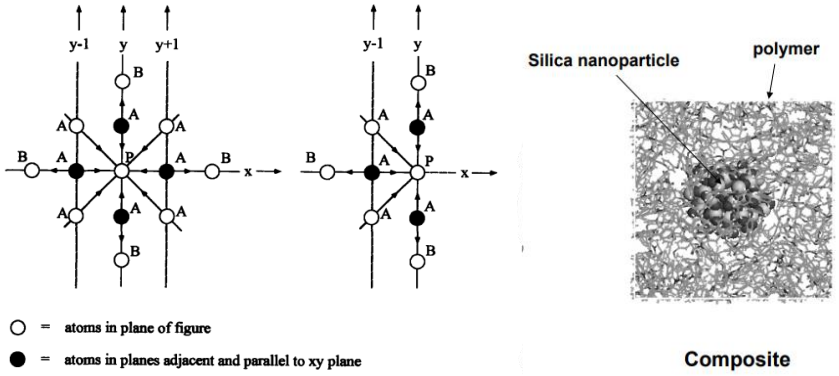


Fig. 1. On the left, an example of the lattice of a metal nanoparticle from [6]; on the right, a Molecular Dynamics simulation of a PMNC with silica filler from [7].

Several **differences** exist between traditional composites and nanocomposites. Assuming the filler is more rigid than the matrix, in bulk composites, particle diameter has little effect on the final elastic modulus; moreover, in some cases, the Young's modulus decreases with the size of particles, as reported by [2] in composites of epoxy and alumina particles with radii of 1, 2, 5, and 8μm. Surface functionalization also does not enhance load transfer [2]. However, when **particle sizes are below 100 nm**, **the behavior is opposite**: smaller particles lead to greater increases in Young's modulus [2], a phenomenon confirmed in several studies [2][8]. Therefore, appropriate models must capture this behavior.

1.2 Simulating the nanoscale

There are two approaches to studying the mechanical properties of nanocomposites.

The first is the **top-down approach**, which involves extending classical continuum mechanics and micromechanics to the nanoscale by incorporating surface and size effects unique to nanomaterials. This method adapts existing theories to

account for how surfaces and interfaces influence the overall mechanical properties of materials. For example, surface elasticity theories have been developed for isotropic materials to consider these surface effects [9]. This approach has been successfully applied to various problems, such as analyzing elastic solids with nanoinclusions or nanocavities [10] and examining the elastic behavior of ultra-thin films [6].

The **bottom-up approach** focuses on building models of nanocomposites from the atomic or molecular level, often using molecular dynamics (MD) simulations to study their mechanical properties. In this method, the interactions between individual atoms or molecules are considered to predict the overall structural behavior [5].

In some cases, these approaches can be used together; for example, Molecular Dynamics can provide useful results for micromechanical analysis when experimental data are not available [12].

The application of nanotechnology offers significant advantages in the fields of structural analysis, thermal insulation, and improved fatigue behavior [41]. The purpose of this research is to provide an overview of existing homogenization models so that bulk data of nanocomposites can be easily derived and used in commercial software, facilitating the work of structural analysts.

In the first section, **semi-empirical theories** will be analyzed. These are simple models developed for bulk composites that, in many cases, have been applied to nanocomposites. In the second section, models based on **variational principles** will be discussed. Thirdly, **Eshelby tensor model** is introduced, which is the most widely used theoretical framework for analyzing the mechanics of nanocomposites. Initially, models considering a spheroidal filler in an infinite medium will be discussed, followed by the case of a finite Representative Volume Element (RVE), and finally models with realistic boundary conditions.

A limitation of the Eshelby tensor approach is that it uses bulk material properties to describe nanoscale phenomena, thereby neglecting **interface effects**. Therefore, in section four, we will introduce additional models that take these effects into account.

Finally, we will reproduce these models and compare them with experimental results from various authors [8][27-40].

Acronym	Meaning
PMNC	Polymeric Matrix Nano-Composite
MMNC	Metal Matrix Nano-Composite
RVE	Representative Volume Element
f	Volume Percentage
w_t	Weight Percentage
X_0	“0” indicates a property of the matrix

$X_{1,2,..}$	"1,2,…" indicate a property of the fillers
$\bar{X}$	The bar indicates a property of the final composite
C	Stiffness tensor
:	Double contraction between tensors
E	Young modulus
ν	Poisson's ratio
G	Shear modulus
K	Bulk modulus
Ω	Volume
$\partial\Omega$	Boundary of the volume

Tab.1: Notation used in the present work.

2 Empirical Models

The following theories are derived from the **interpolation of experimental data**. These models typically assume idealized conditions, such as perfect adhesion between the filler and matrix, as well as the complete dispersion of individual filler particles. **Einstein's equation** was originally formulated to describe the effective shear viscosity of dilute suspensions of rigid spheres:

$$\bar{E} = E_0(1 + 2.5f) \tag{1}$$

In this equation, $\bar{E}$ and E_0 denote the Young's modulus of the composite and the matrix, respectively, while f represents the particle volume fraction. This equation is valid only for low filler concentrations and predicts a linear relationship between $\bar{E}$ and f, independent of particle size. However, at higher concentrations, interactions between the strain fields surrounding the particles lead to inaccuracies in the model's predictions [2]. To address this, **Guth** introduced a particle interaction term, modifying Einstein's equation to:

$$\bar{E} = E_0(1 + 2.5f + 14.1f^2) \tag{2}$$

In this formulation, the linear term represents the stiffening effect of individual particles, while the quadratic term accounts for particle interactions [2]. Both formulations do not include the influence of the stiffness of the inclusions but only their concentration.

The **Halpin-Tsai** equation is used to model composites containing short fibers. In this model, the aspect ratio of the filler is first calculated. The elastic modulus in the fiber direction is then given by [12]:

$$\overline{E_{11}} = E_0\left(\frac{1+\eta\xi f_1}{1-\eta f_1}\right)$$
$$\eta = \frac{\frac{E_1}{E_0}-1}{\frac{E_1}{E_0}+\xi} \tag{3}$$

where $\xi = \frac{2l}{d}$, l represents the fiber length and d is the diameter. For nanoparticles, $\overline{E_{11}} = \bar{E}$ can be assumed. For instance, this formula has been employed to derive the elastic properties of nanocomposites composed of spherical particles in homogenized finite element models [13].

3 Models from Variational principles

Several models are derived from variational principles, such as the principle of minimum potential energy. In these models, displacement boundary conditions are applied to the boundary $\partial\Omega$ of the volume Ω of the material. The macroscale potential energy density $W(\varepsilon)$ is defined as:

$$W(\varepsilon) = \frac{1}{2\Omega}\int_{\Omega} C_{ijkl}\varepsilon_{ij}\varepsilon_{kl}d\Omega \tag{4}$$

where ε_{ij} represents the strain using Einstein's notation. Within this framework, the **Voigt** model is the well-known "rule of mixtures" for composite materials. For a composite with a single type of filler, it is expressed as:

$$\bar{E} = f_0E_0 + f_1E_1 \tag{5}$$

where f_0 denotes the volume fraction of the matrix and f_1 the volume fraction of the filler. In the Voigt model, this equation provides an upper bound for the effective modulus of composite materials [14].

By applying the complementary strain energy principle, the **Reuss** model, or lower bound predictor, can be obtained:

$$\frac{1}{\bar{E}} = \frac{f_0}{E_0} + \frac{f_1}{E_1} \tag{6}$$

This model represents the lower bound of the effective modulus [14]. The same equations (4) and (5) can be applied to the full elastic stiffness tensor. Other boundary models are the Hashin-Shtrikman bounds [18].

4 Models from Eshelby's formulation

4.1 Eshelby's tensor on Infinite RVE

The **Eshelby** model serves as the foundation for numerous analytical approaches. Eshelby considers an elastic medium containing inclusions, assuming perfect bonding between the matrix and inclusions. The matrix is treated as infinitely large relative to the inclusions, such that from the perspective of the inclusions, the medium appears infinite. Additionally, the inclusions are assumed to be well-dispersed and non-interacting, allowing for the assumption of an "infinite representative volume element (RVE)" surrounding each inclusion. Under these assumptions, the model proceeds through the following virtual operations:

- Start with the composite consisting of both the matrix and fillers.
- Virtually remove the fillers, allowing the matrix to relax into the voids created.
- Apply surface tractions to the voids to restore their original shape; for instance, if shrinkage occurs after filler removal, the surface traction enlarges the void to its initial size.
- Finally, the voids are virtually refilled with the matrix material, rather than the composite [15].

The result is a composite where the stiffness tensor of the matrix can be legitimately used, as the matrix remains the only constituent in this virtual operation. However, eigenstrains are applied to the regions where the fillers were originally located [16]:

$$\varepsilon_{ij}^{*}(\boldsymbol{x}) = \begin{cases} \varepsilon_{ij}^{*}, & x \in \Omega_1 \\ 0, & x \in \Omega/\Omega_1 \end{cases} \tag{7}$$

where Ω_1 represents the volume of the filler, and Ω is the volume of the infinite RVE surrounding the filler. The purpose of Eshelby's method is to find a tensor that relates the strain in the material to the eigenstrain [16]:

$$\varepsilon_{ij}^{d}(\boldsymbol{x}) = \mathbb{S}_{ijkl}^{\infty}(\boldsymbol{x})\varepsilon_{kl}^{*} \tag{8}$$

In this equation, ε_{ij}^{d} denotes the strain in the homogenized material, ε_{kl}^{*} the eigenstrain, and $\mathbb{S}_{ijkl}^{\infty}$ the Eshelby tensor (with "∞" signifying the infinite RVE). Eshelby provides an **exact**, **closed-form solution** for the problem, offering values for the **interior** (I) Eshelby tensor $\mathbb{S}_{ijkl}^{I,\infty}$ (which applies to the volume Ω_1 inside the filler) and the **exterior** Eshelby tensor $\mathbb{S}_{ijkl}^{E,\infty}$ (which applies outside the inclusion, that is Ω/Ω_1). Here it is reported the equation for interior Eshelby tensor in 2D problem [16], see [16] for the exterior Eshelby tensor:

$$\mathbb{S}_{ijkl}^{I,\infty}(\boldsymbol{x}) = \frac{(3-4\upsilon)}{8(1-\upsilon)}(\delta_{ik}\delta_{jl} + \delta_{il}\delta_{jk}) + \frac{(4\upsilon-1)}{8(1-\upsilon)}\delta_{ij}\delta_{kl}, \quad \boldsymbol{x} \in \Omega_1 \tag{9}$$

It is important to note that the value of the interior Eshelby tensor is spatially constant, ensuring that the eigenstrain remains uniform inside the inclusion. In contrast, the exterior Eshelby tensor is not constant.

4.2 Mori-Tanaka method

The **Mori-Tanaka** method utilizes the Eshelby tensor derived from an infinite representative volume element (RVE) to determine the homogenized stiffness tensor of a composite material [17]. The assumptions underlying this model are that the composite consists of two perfectly bonded phases (matrix and filler), with the filler being well dispersed throughout the matrix. Additionally, it is assumed that no inclusions are located near the boundaries of the matrix, thus avoiding boundary effects [17].

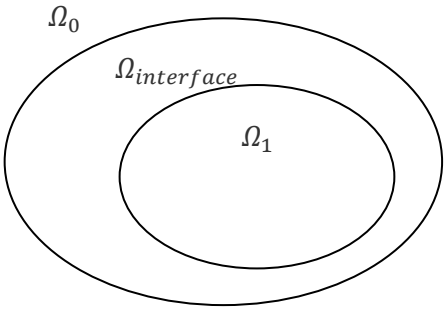


Fig. 2. Scheme for Mori-Tanaka lemma; the fluctuation stress is present only in an interface zone and vanishes if the distance from the inclusion increases.

The method is based on the **Mori-Tanaka lemma**, which states that if the composite is subjected to far-field stress, the stress in the matrix near an inclusion is equal to the far-field stress plus fluctuations caused by the presence of the inclusion. These fluctuations diminish as the distance from the inclusion increases [17][18]. Using this principle, it is possible to derive the first estimation of the homogenized stiffness tensor for the composite [7]:

$$\begin{aligned} C &= (f_0 C_0 + f_1 C_1 : T_1) : (f_0 I + f_1 T_1)^{-1} \\ T_1 &= \left(I + \mathbb{S}^{I,\infty} : C_0^{-1} : (C_1 - C_0)\right)^{-1} \end{aligned} \tag{10}$$

In this equation, I represents the fourth-order identity tensor, f the volume percentage of matrix or filler and T_1 is the dilute strain concentration tensor.

Several authors have proposed simplified expressions based on this model. For instance, [2] provides the following formula for the composite's elastic modulus:

$$\bar{E} = \frac{9\bar{K}\bar{G}}{3\bar{K}+\bar{G}} \tag{11}$$

where $\bar{K}$ is the bulk modulus and $\bar{G}$ is the shear modulus. A similar expression is derived by [19], who demonstrates the connection between their micromechanical formulation, the Mori-Tanaka method, and the Hashin-Shtrikman bounds.

4.3 Eshelby's tensor on Finite RVE

The previously discussed models assume that the Eshelby tensor is computed in an infinite representative volume element (RVE), which results in the omission of geometrical parameters, such as the size of the filler, in the final formulation. In contrast, [16] introduces the concept of the Eshelby tensor within a finite RVE. The hypothesis is that both the inclusion and the surrounding RVE are circular or spherical in shape (see figure 3).

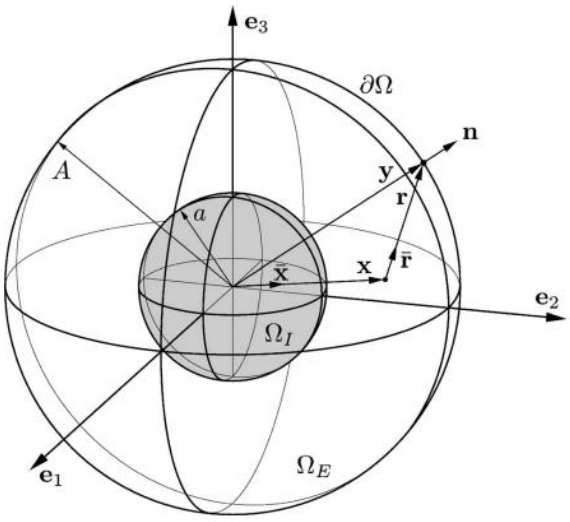


Fig. 3. Spherical Representative Volume Element from [26]

First, [16] decomposes the classical infinite RVE Eshelby solution into a basis of circular coordinates:

$$\Theta_{ijkl}(\boldsymbol{r}) = \begin{bmatrix} \delta_{ij}\delta_{kl} \\ \delta_{ik}\delta_{jl} + \delta_{il}\delta_{jk} \\ \delta_{ij}r_k r_l \\ \delta_{kl}r_i r_j \\ r_i r_j r_k r_l \end{bmatrix} \tag{12}$$

Given that the RVE is finite and circular, they hypothesize a **radially symmetric solution**. Under this assumption, a closed-form solution for the Eshelby tensor is

derived. In this case, the presence of **boundary conditions alters the form of the solution**, yielding different results depending on whether Dirichlet or Neumann boundary conditions are applied [16]. For the complete expression of the Eshelby tensor in a finite RVE under Dirichlet boundary conditions, see equation (57) in [16]. Moreover, [20] presents expressions for the Eshelby tensor in a three-dimensional spherical finite RVE under both Dirichlet and Neumann boundary conditions.

The final solution consists of a constant dilatational part and a term that depends on the radius of the RVE; as this radius approaches infinity, the solution converges to the Eshelby tensor for an infinite RVE, as described in previous models. To achieve proper homogenization, spatial averaging is required. For Dirichlet boundary conditions, the following formulas are obtained [20]:

$$\begin{aligned}\langle \mathbb{S}^{I,\blacksquare}_{ijkl} \rangle_{\Omega_I} &= s_1^{I,\blacksquare} \mathbb{E}^{(1)}_{ijkl} + s_2^{I,\blacksquare} \mathbb{E}^{(2)}_{ijkl} \\ \langle \mathbb{S}^{E,\blacksquare}_{ijkl} \rangle_{\Omega_E} &= s_1^{E,\blacksquare} \mathbb{E}^{(1)}_{ijkl} + s_2^{E,\blacksquare} \mathbb{E}^{(2)}_{ijkl}\end{aligned} \tag{13}$$

where $\mathbb{E}$ represents the E-bases and ■ stands for Dirichlet (D) or Neumann (N) boundary conditions. Consult equations (8-14) of [20] for the full expressions. The resulting estimation of the stiffness tensor is given by [20]:

$$\begin{aligned}\bar{C} &= C_0 - f C_0 : \left(A - \langle \mathbb{S}^{I,D} \rangle_{\Omega_I} \right)^{-1} \\ A &= (C_0 - C_1)^{-1} : C\end{aligned} \tag{14}$$

In practical scenarios, a combination of Dirichlet and Neumann boundary conditions is often observed, representing conditions on displacement and force, respectively. [21] proposes a linear combination of these boundary conditions:

$$\mathbb{S}^{\sharp,F} = \alpha \mathbb{S}^{\sharp,D}(\boldsymbol{x}) + (1-\alpha)\mathbb{S}^{\sharp,N}(\boldsymbol{x}) \tag{15}$$

where ♯ stands for interior (I) or exterior (E) Eshelby tensor, "F" indicates the composition of boundary condition, "D" the Dirichlet boundary condition, "N" the Neumann boundary condition and α is a coefficient in the range from 0 to 1. With this new expression for the averaged Eshelby tensor, it becomes possible to refine the Mori-Tanaka equation, therefore the estimation of stiffness tensor results in [20]:

$$\bar{C} = C_0 - f_0 C_0 : \left(A - (1-f) \left(\langle \mathbb{S}^{I,F} \rangle_{\Omega_I} - \langle \mathbb{S}^{E,F} \rangle_{\Omega_E} \right) \right)^{-1} \tag{16}$$

For the full expression of the combined boundary conditions, refer to [21].

5 Interface Models

A key limitation of the Eshelby model is its reliance on the bulk properties of materials, without accounting for the interface effects, which are critical to the final properties of nanocomposites [10]. As previously discussed, the **interface** plays a crucial role in determining the mechanical behavior of nanocomposites. The first study of surface stress, conducted by Gurtin and Murdoch [9], developed a framework to account for stress and strain in elastic bodies. Building on this, [10] applied their formulation to study stress in nanopores using an energetic approach, minimizing the free energy of a symmetrical RVE with a spherical inclusion, modeled as a void. In [22], the double-inclusion model is introduced, wherein the interface is treated as a shell surrounding the nanoparticle. This model assumes perfect bonding between the three phases (matrix, nanoparticles, and interphase) and applies the Eshelby formulation to all phases. However, no special conditions are applied to the shell, with the claim that it does not significantly affect the estimation of the composite's final stiffness. A similar approach is adopted by [23], who propose an "interlayer domain" model, suggesting that the Eshelby tensor for the interface is identical to that for the inclusion's interior.

Another important study on interface properties is provided by [7]. This work suggests that the zone between the filler and matrix involves a mixture of their respective molecules and constituents, justifying the introduction of an "interphase" layer. The geometric and elastic properties of this interphase are determined using Molecular Dynamics (MD) simulations, after which the micromechanical model of [24] is used by [7] to compute the composite's final properties:

$$\bar{C} = C_0 + \big((f_1 + f_2)(C_2 - C_0){:}T_2 + f_1(C_1 - C_2){:}T_1\big)(f_0 I + (f_1 + f_2)T_2)^{-1} \quad (17)$$

where “2” indicates the interphase. Simulations show that as the particle radius increases, the effect of the interface on the final stiffness decreases. This finding aligns with the surface stress hypothesis introduced in [6]: as the surface-to-volume ratio decreases, the Young’s modulus approaches the value predicted by the Mori-Tanaka model.

Until now, we have assumed perfect bonding between the matrix, interface, and inclusion. However, [25] classifies three different interface models:

- The **free sliding** model, where normal traction and displacement at the interface are continuous, but shear traction is neglected.
- The **linear spring** model, in which the interface behaves like a linear spring in both tangential and normal directions.
- The **dislocation-like** model, similar to the linear spring model, but where displacement in one direction is proportional to displacement in another direction.

- The **interface stress** model, which treats the interface as an independent phase, as in previous studies by [7][23][22].

Here some details about interface stress model are reported. The mathematical formulation is given as:

$$\begin{cases} [u] = 0 \\ n \cdot [\sigma] \cdot n = -\tau : \kappa \\ P \cdot [\sigma] \cdot n = -\nabla_s \cdot \tau \end{cases} \tag{17}$$

where $P{=}I^{(2)} - n{\otimes}n$, $I^{(2)}$ is the second order identity tensor, n represents the normal of the surface, κ is the curvature tensor, τ is the interface stress tensor, and $\nabla_s \cdot \tau$ represents the divergence of the tensor field [9]. The interface stress follows a linear elastic approach and can be expressed in terms of Lame constants:

$$\tau = 2\lambda_s E + \mu_s tr(\mathrm{E})I \tag{18}$$

where λ_s and μ_s are the **interface moduli** and E represents the strain tensor. Building on this, [25] extends the Eshelby model to incorporate these interface moduli, and [5] performs the necessary averaging, demonstrating the dependence of the final elastic modulus on nanoparticle radius, volume fraction, and interface moduli.

This model is one of the most complex currently used, as it incorporates every parameter of the composite—nanoparticle radius, volume, bulk properties, and interface moduli. For instance, it accurately predicts that a decrease in nanoparticle radius leads to an increase in the composite's Young's modulus.

The interface moduli are a key measure of how well-bonded the matrix and nanofiller are. Bulk properties can be measured in separate experiments, however, interface moduli require to have already the final composite. As a consequence, the method is not well-suited for full "a priori" estimation. At the same time, [11] performs a fitting of the Birch-Murnaghan energy equation to MD results in order to determine the interface moduli of specific nanocomposites, instead of conducting practical experiments.

6 Comparison with experimental results

Table 2 gathers experimental data from literature.

Matrix	*Filler*	E_0 (GPa)	υ_0	E_1 (GPa)	υ_1	f_1	$\bar{E}$ (GPa)	Sources
Nylon-6	SiO_2	1.30	0.41	73	0.17	1%	1.65	[27][28]
Nylon-6	SiO_2	1.30	0.41	73	0.17	2%	1.88	[27]
PEEK	SiO_2	3.9	0.356	88.7	0.082	2.5%	4.1	[30]
PEEK	SiO_2	3.9	0.356	88.7	0.082	5%	4.1	[30]
PEEK	SiO_2	3.9	0.356	88.7	0.082	7.5%	4.3	[30]

Epoxy	SiO_2	3.30	0.41	73.1	0.17	0.3%	3.4	[31] [29]
Epoxy	SiO_2	3.30	0.41	73.1	0.17	1.6%	3.43	[31] [27]
Epoxy	SiO_2	3.30	0.41	73.1	0.17	3%	3.67	[31] [27]
Epoxy Epon 862	SiO_2 *R=80nm*	2.830	0.3	70	0.28	0.55%	2.83	[8]
Epoxy Epon 862	SiO_2 *R=80nm*	2.830	0.3	70	0.28	0.82%	2.97	[8]
Epoxy Epon 862	SiO_2 *R=80nm*	2.830	0.3	70	0.28	1.63%	3.12	[8]
Epoxy Epon 862	SiO_2 *R=20nm*	2.830	0.3	70	0.28	0.55%	3.09	[8]
Epoxy Epon 862	SiO_2 *R=20nm*	2.830	0.3	70	0.28	0.82%	3.10	[8]
Epoxy Epon 862	SiO_2 *R=20nm*	2.830	0.3	70	0.28	1.63%	3.14	[8]
Al	*TiC*	68	0.33	460	0.18	17%	108	[32]
Al	*TiC*	68	0.33	460	0.18	35%	200	[32]
AA6063	TiO_2	70	0.3	259	0.28	3%	70.3	[33][36]
AA6063	TiO_2	70	0.3	259	0.28	5%	70.8	[33][36]
AA6063	TiO_2	70	0.3	259	0.28	7%	71	[33][36]
AZ31	Al_2O_3	45	0.33	417	0.27	1.5%	49	[34][37]
AZ91	Al_2O_3	55.3	0.35	314	0.27	1.5%	58.6	[35][37]

Table 2. Collection of experimental data of stiffness of nanocomposites.

Under the hypothesis of linear elastic materials (for matrix, nanoinclusions and interface), Young modulus is computed using different methods shown in the present work: Figure 4 shows the percentage error (absolute value) for each type of nanocomposites. On Y axis, the average percentage error is reported, by assuming the experimental data as the true value.

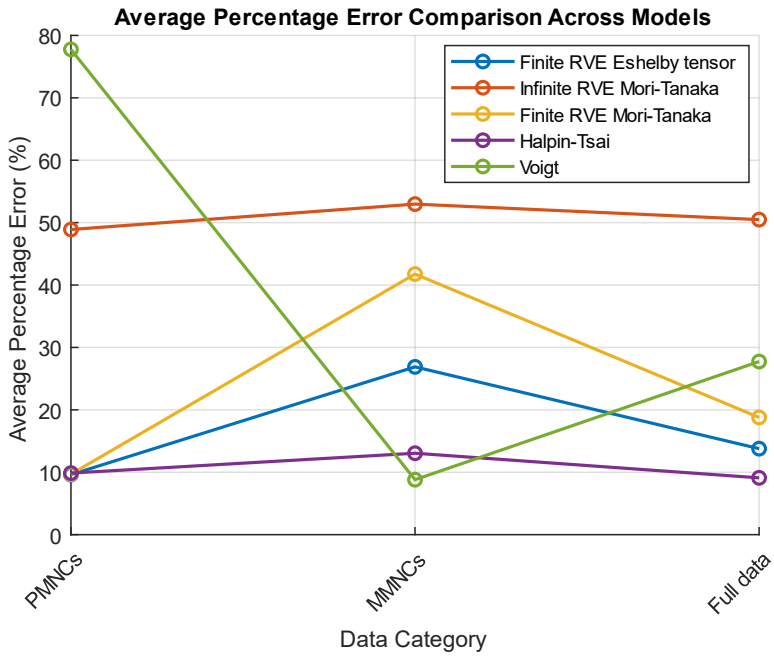


Fig. 4. Comparison of homogenization methods with class of nano-composite materials; PMNCs stands for "Polymer Matrix Nano-Composites", "MMNCs" stands for "Metal Matrix Nano-Composites". The results are expressed in absolute values.

7 Discussion

The purpose of this work is to provide a holistic overview of analytical methods for the homogenization of nanocomposite materials.

Regarding traditional methods, the Voigt rule (Equation (5)) is generally not suitable in most cases, except for Metal Matrix Nanocomposites (MMNCs), where it performs well with an average relative error of 8.80%. The Halpin-Tsai rule (Equation (3)) performs better for Polymeric Matrix Nanocomposites (PMNCs), with an error of 9.86%. Both methods are easy to apply and can serve as valid approaches for homogenization.

Concerning methods derived from the Eshelby tensor, The Mori-Tanaka method, in its traditional form (equation (10)), proves inadequate for nanocomposites due to the large errors computed. In contrast, the refined Mori-Tanaka method (employing the Finite Representative Volume Element (RVE) Eshelby tensor, equation (16)) provides better estimations. The errors are comparable to those of the Finite RVE Eshelby tensor method under Dirichlet boundary conditions (equation (14)), as the mathematical foundations are the same. The Finite RVE Eshelby tensor with Dirichlet boundary conditions represents the best approach to estimate the stiffness of PMNCs, achieving an absolute percentage error of 9.61%.

The effectiveness of the Interface Stress Model depends on the calculation of interface moduli, which require the use of Molecular Dynamics simulations [40] or inference from experimental results. Consequently, the method is not viable when computational time is a critical concern. Furthermore, only two experimental data points are available; thus, its application was not considered in this analysis.

In conclusion, traditional methods can provide good estimations of the final stiffness of materials, but more refined methods, such as those based on the Eshelby tensor and interface stress, are better capable of simulating the variation of design parameters in nanocomposites.

8 Acknowledgments

This publication is part of the project PNRR-NGEU which has received funding from the MUR – DM 117/2023.



References

[1] Agrawal D.C. (2013) Introduction to Nanoscience and Nanomaterials. World Scientific, 556 pages, ISBN 978-981-4397-97-1.

[2] Fu S.-Y., Feng X.-Q., Lauke B., Mai Y.-W. (2008) Effects of particle size, particle/matrix interface adhesion and particle loading on mechanical properties of particulate–polymer composites. Composites Part B: Engineering 39(6):933–961. https://doi.org/10.1016/j.compositesb.2008.01.002.

[3] Cao G. (2004) Nanostructures and Nanomaterials. Imperial College Press, London.

[4] Khan I., Saeed K., Khan I. (2019) Nanoparticles: Properties, applications and toxicities. Arabian Journal of Chemistry 12(7):908–931. https://doi.org/10.1016/j.arabjc.2017.05.011.

[5] Kim B.R., Pyo S.H., Lemaire G., Lee H.K. (2011) Multiscale approach to predict the effective elastic behavior of nanoparticle-reinforced polymer composites. Interaction and Multiscale Mechanics 4(3):173–185. https://doi.org/10.12989/imm.2011.4.3.173.

[6] Cammarata R.C. (1994) Surface and interface stress effects in thin films. Progress in Surface Science 46(1):1–38. https://doi.org/10.1016/0079-6816(94)E0001-Z.

[7] Odegard G.M., Clancy T.C., Gates T.S. (2005) Modeling of the mechanical properties of nanoparticle/polymer composites. Polymer 46(2):553–562.

[8] Jang J.-S., Bouveret B., Suhr J., Gibson R.F. (2012) Combined numerical/experimental investigation of particle diameter and interphase effects on coefficient of thermal expansion and Young's modulus of SiO_2/epoxy nanocomposites. Polymer Composites 33(8):1415–1423

[9] Gurtin M.E., Murdoch I. (1975) A continuum theory of elastic material surfaces. Archive for Rational Mechanics and Analysis 57(4):291–323. https://doi.org/10.1007/BF00261375.

[10] Sharma P., Ganti S., Bhate N. (2003) Effect of surfaces on the size-dependent elastic state of nano-inhomogeneities. Applied Physics Letters 82(4):535–537. https://doi.org/10.1063/1.1539929.

[11] Yang B.J., Shin H., Lee H.K., Kim H. (2013) A combined molecular dynamics/micromechanics/finite element approach for multiscale constitutive modeling of nanocomposites with interface effects. Applied Physics Letters 103(24):241903. https://doi.org/10.1063/1.4819383.

[12] Halpin J.C. (1969) Stiffness and expansion estimates for oriented short fiber composites. Journal of Composite Materials 3(4):732–734. https://doi.org/10.1177/002199836900300419.

[13] Zhao B., Zhao Y., Shen Y., He H., Qu Z. (2023) Numerical simulation and comparison of the mechanical behavior of toughened epoxy resin by different nanoparticles. ACS Omega 8(34):31123–31134. https://doi.org/10.1021/acsomega.3c03093.

[14] Li S., Wang G. (2018) Introduction to Micromechanics and Nanomechanics. 2nd edn. World Scientific, 660 pages. https://doi.org/10.1142/8644.

[15] Eshelby J.D. (1957) The determination of the elastic field of an ellipsoidal inclusion, and related problems. Proceedings of the Royal Society of London. Series A 241:376–396. https://doi.org/10.1098/rspa.1957.0133.

[16] Li S., Sauer R., Wang G. (2005) A circular inclusion in a finite domain I. The Dirichlet-Eshelby problem. Acta Mechanica 179(1-2):67–90. https://doi.org/10.1007/s00707-005-0234-2.

[17] Mori T., Tanaka K. (1973) Average stress in matrix and average elastic energy of materials with misfitting inclusions. Acta Metallurgica 21(5):571–574. https://doi.org/10.1016/0001-6160(73)90064-3.

[18] Benveniste Y. (1987) A new approach to the application of Mori-Tanaka's theory in composite materials. Mechanics of Materials 6(2):147–157. https://doi.org/10.1016/0167-6636(87)90005-6.

[19] Ju J.W., Chen T.M. (1994) Micromechanics and effective moduli of elastic composites containing randomly dispersed ellipsoidal inhomogeneities. Acta Mechanica 103:103–121. https://doi.org/10.1007/BF01180221.

[20] Li S., Wang G., Sauer R.A. (2007) The Eshelby tensors in a finite spherical domain—Part II: Applications to homogenization. Journal of Applied Mechanics 74(4):784–797. https://doi.org/10.1115/1.2711228.

[21] Sauer R.A., Wang G., Li S. (2008) The composite Eshelby tensors and their applications to homogenization. Acta Mechanica 197:63–96. https://doi.org/10.1007/s00707-007-0504-2.

[22] Hori M., Nemat-Nasser S. (1993) Double-inclusion model and overall moduli of multi-phase composites. Mechanics of Materials 14(3):189–206. https://doi.org/10.1016/0167-6636(93)90066-Z.

[23] Liu H.T., Sun L.Z. (2005) Multi-scale modeling of elastoplastic deformation and strengthening mechanisms in aluminum-based amorphous nanocomposites. Acta Materialia 53(9):2693–2701. https://doi.org/10.1016/j.actamat.2005.02.029.

[24] Dunn M.L., Ledbetter H. (1995) Elastic moduli of composites reinforced by multiphase particles. Journal of Applied Mechanics 62(4):1023–1028. https://doi.org/10.1115/1.2896038.

[25] Duan H.L., Wang J., Huang Z.P., Luo Z.Y. (2005) Stress concentration tensors of inhomogeneities with interface effects. Mechanics of Materials 37(7):723–736. https://doi.org/10.1016/j.mechmat.2004.07.004.

[26] Li S., Sauer R.A., Wang G. (2007) The Eshelby tensors in a finite spherical domain—Part I: Theoretical formulations. Journal of Applied Mechanics 74(4):770–783. https://doi.org/10.1115/1.2711227.

[27] Hasan M.M., Zhou Y., Mahfuz H., Jeelani S. (2006) Effect of SiO_2 nanoparticle on thermal and tensile behavior of nylon-6. Materials Science and Engineering: A 429(1-2):181–188. https://doi.org/10.1016/j.msea.2006.05.124.

[28] Yang B.J., Hwang Y.Y., Lee H.K. (2013) Elastoplastic modeling of polymeric composites containing randomly located nanoparticles with an interface effect. Composite Structures 99:123–130. https://doi.org/10.1016/j.compstruct.2012.11.043.

[30] Kuo M.C., Tsai C.M., Huang J.C., Chen M. (2005) PEEK composites reinforced by nano-sized SiO_2 and Al_2O_3 particulates. Materials Chemistry and Physics 90(1):185–195. https://doi.org/10.1016/j.matchemphys.2004.10.009.

[31] Gao J., Li J., Benicewicz B.C., Zhao S., Hillborg H., Schadler L.S. (2012) The mechanical properties of epoxy composites filled with rubbery copolymer grafted SiO_2. Polymers 4(1):187–210. https://doi.org/10.3390/polym4010187.

[32] Lin T.C., Cao C., Sokoluk M., et al. (2019) Aluminum with dispersed nanoparticles by laser additive manufacturing. Nature Communications 10:4124. https://doi.org/10.1038/s41467-019-12047-2.

[33] Jaber M.H., Aziz G.A., Mohammed A.J., AL-AIKawi H.J. (2020) Electrical conductivity, magnetic and fatigue properties of aluminum matrix composites reinforced with nano-titanium dioxide (TiO_2). Nanocomposites 6(2):47–55. https://doi.org/10.1080/20550324.2020.1769976.

[34] Arun J., Raj T.G.A., Roy K.E.R., Suresh S. (2022) Fatigue life, distortion behavior of AA 8011-nano B_4C composite using simulated acoustic emission technique – An experimental and statistical appraisal. International Journal of Fatigue 164:107168. https://doi.org/10.1016/j.ijfatigue.2022.107168.

[35] Srivatsan T.S., Godbole C., Paramsothy M., Gupta M. (2012) The role of aluminum oxide particulate reinforcements on cyclic fatigue and final fracture behavior of a novel magnesium alloy. Materials Science and Engineering: A 532:196–211. https://doi.org/10.1016/j.msea.2011.10.081.

[36] AZoM., Titanium Dioxide - Titania (TiO_2). Retrieved from https://www.azom.com/properties.aspx?ArticleID=1179.

[37] AZoM., Alumina - Aluminium Oxide (Al_2O_3) - A Refractory Ceramic Oxide. Retrieved from https://www.azom.com/properties.aspx?ArticleID=52.

[38] Dongdong Gu, Hongqiao Wang, Donghua Dai, Pengpeng Yuan, Wilhelm Meiners, and Reinhart Poprawe. Rapid fabrication of al-based bulk-form nanocomposites with novel reinforcement and enhanced performance by selective laser melting. Scripta Materialia, 96:25–28, 2015.

[39] Tianqi Wang, Qingshi Meng, Sherif Araby, Guang Yang, Pengxu Li, Rui Cai, Sensen Han, and Wei Wang. Non-oxidized graphene/metal composites by laser deposition additive manufacturing. Journal of Alloys and Compounds, 882:160724, 2021.

[40] Zhu Y., Hu X., Ni Y. (2021) Molecular dynamics simulation of microstructure evolution during the fracture process of nano-twinned Ag. Engineering Fracture Mechanics 248:107743. https://doi.org/10.1016/j.engfracmech.2021.107743.

[41] Cestino E., Catapano J., Galvano F., Felis A., Zuccalà S., Martilla V., Sapienza V., Chesta L. (2024) Effectiveness of nanotechnology treatments in composite aircraft applications. Applied Sciences 14(5):1721. https://doi.org/10.3390/app14051721.